# H atom in $BaTiO_3$ and $CaTiO_3$ crystals: structure, electronic properties and diffusion

Johnny Chimborazo*, Milagros Castillo, Carmen Velasco, Arvids Stashans

Centro de Investigación en Física de la Materia Condensada, Corporación de Física Fundamental y Aplicada, Apartado 17-12-637, Quito, Ecuador

## ABSTRACT

We investigate effects that an H impurity produces upon the geometry and the electronic structure in the $BaTiO_3$ and $CaTiO_3$ crystals considering several lattices of these materials. In order to study the H-doped barium and calcium titanates we use a quantum-chemical method based on the Hartree-Fock formalism and a periodic large unit cell (LUC) model. As a result, the interstitial H is found to bind to one of the O atoms forming the so-called OH group. In equilibrium, O-H distance is found to be 0.89 and 0.91 Å for $BaTiO_3$ cubic and tetragonal lattices, respectively. These results thus predict reduction of the O-H bond-length compared to a free radical, obviously due to rather compact crystalline lattice. In the case of the $CaTiO_3$ crystals, the O-H distance is found to be 0.89 and 1.04 Å for cubic and orthorhombic phases, respectively. We also study the impurity effect upon the lattice distortion and analyze the ferroelectric polarization in the tetragonal $BaTiO_3$. A qualitative study shows that the absolute values of the effective charges decrease while the Ti-O bond-lengths increase considerably in the defective region. Combining these two effects we obtain that the bulk ferroelectric polarization increases 1.27 times. Therefore, one can conclude that the ferroelectric degradation is not a bulk effect. This could also provide an explanation for the oxygen loss in the ferroelectric films near the surface under thermal annealing in hydrogen atmosphere. Diffusion of the hydrogen in the $BaTiO_3$ cubic lattice is also studied in the present work considering different types of trajectories. The diffusion path that gives the lowest potential energy barrier for the hydrogen motion is found to be of a parabolic form.

**Keywords:** $BaTiO_3$, $CaTiO_3$, H impurity, Hartree-Fock formalism

## 1. INTRODUCTION

An important class of ceramic materials known as perovskites is of great scientific and technological interest due to their unusual properties. Ferroelectric and piezoelectric perovskite-type titanates, $BaTiO_3$ and $CaTiO_3$, are of a special interest. $BaTiO_3$ presents a large electro-optic coefficient and high photorefractive sensitivity and is a promising material for self-pumped phase conjugation holographic storage and inexpensive diode lasers.[1-3] $CaTiO_3$ is one of the important constituents for the disposal of high level radioactive waste materials and is also utilized in the construction of field devices and sensors.[4] It is known that titanates are strongly influenced by presence of point defects and although different properties of $BaTiO_3$ and $CaTiO_3$ crystals originated due to the defects are not studied sufficiently.

In the present work we study the effects that an H impurity produces upon the geometry and electronic structure of the $BaTiO_3$ cubic and tetragonal lattices as well as $CaTiO_3$ cubic and orthorhombic crystallographic lattices. Atomic displacements and relaxation energies are comparatively analyzed for each crystal.

## 2. METHOD

In the present research we use the Hartree-Fock method based on the molecular orbital (MO) theory and the periodic LUC model. The periodicity condition and a careful treatment of the exchange interaction make to this approach very reliable in study of the electronic band structure and calculation of the total energy for a given system. Although the main computational equations and the fundamentals for the total energy calculations have been described extensively elsewhere,[5,6] it is useful to point out the basic idea of the LUC formalism, the so-called $k = 0$ approximation. The self-consistency of the Fock matrix elements in this approach is achieved by obtaining the density matrix elements in the following manner:

$$P^0_{pq} = \frac{1}{N}\sum_k P_{pq}(\boldsymbol{k})\exp(i\boldsymbol{k}\boldsymbol{R}_v) \quad (1)$$

Here, the summation is carried out over all $k$ values in the reduced Brillouin zone (BZ) of the LUC. The information obtained corresponds only to the point $k$ = 0 of the density matrix, $P_{pq}(\boldsymbol{k})$. Nevertheless, it has been proven that this is equivalent to a band structure calculation at those $k$ points, which transform to the reduced BZ center after the extension of the primitive unit cell. Usually eight-fold or even four-fold-symmetric extension proves to be sufficient[7-10] to reproduce correctly the electronic band structure and the geometry of a given crystal. In our case, the eight-fold (2x2x2) extended LUC consisting of 40 atoms was exploited to study H impurity in the cubic and tetragonal phases of $BaTiO_3$ crystal and $CaTiO_3$ cubic phase while for studies of $CaTiO_3$ orthorhombic phase 80 atom LUC was used. We can state that the current method has been applied successfully to study different titanates. Some examples include calculation of hole self-trapping in $BaTiO_3$[11-13] and $SrTiO_3$[14] crystals, impurity doping in $BaTiO_3$,[15-18] $SrTiO_3$,[10,19,20] $CaTiO_3$,[21-23] and $PbTiO_3$[24] materials and another studies.

## 3. RESULTS AND DISCUSSION

### 3.1. O-H bonding in $BaTiO_3$ crystals

In order to find the energy-minimum configuration, we have investigated a number of possible sites for the H intercalation. Afterwards, the geometry optimization, including the automated geometry optimization procedure using the downhill simplex method in multidimensions, was applied. As a result, the obtained H-equilibrium position is shown in Fig. 1.

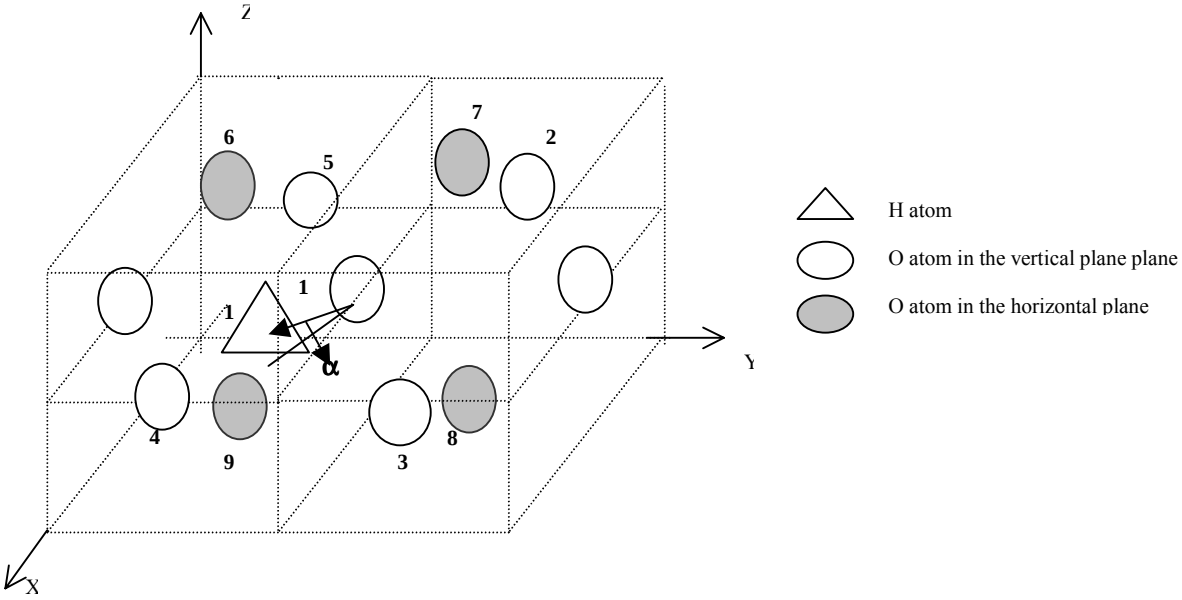


**Fig. 1.** A schematic diagram describing the H equilibrium position in the $BaTiO_3$ crystals. White and gray spheres indicate O atoms located in the middle of vertical and horizontal planes, respectively. The impurity atom is located just above the plane formed by O(2), O(3), O(4) and O(5) atoms and forms an angle α with this plane. α = 4.00º and 8.76º for the cubic and tetragonal lattices, respectively.

The calculated distance of the O-H bond-length is found to be equal to 0.89 Å and 0.91 Å in the cubic and tetragonal phases, respectively. Thus one can notice that the obtained bond-length magnitudes are smaller than the bond length of a free $OH^-$ group, 0.97 Å. We justify the shorter bond-length for the $OH^-$ complex within the crystalline structure due to rather compact crystalline packing in the $BaTiO_3$ crystals.

### 3.2. Lattice response to the H-impurity in $BaTiO_3$

The crystalline lattice is perturbed by the impurity presence, and as a result the defect-closest atoms move to their new equilibrium sites. The change in atomic positions in the cubic structure of the $BaTiO_3$ is shown in Fig. 2. The two Ti atoms

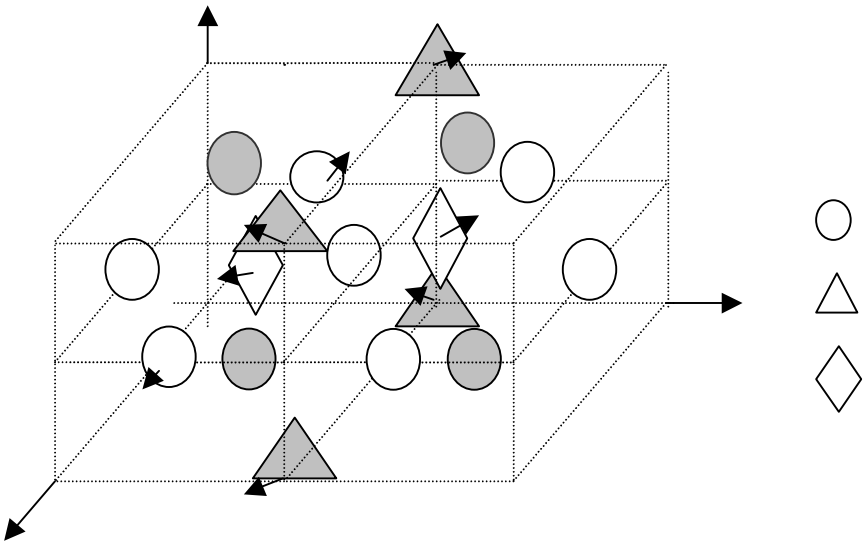

**Fig. 2.** Lattice relaxation in the $BaTiO_3$ cubic phase. The arrows show defect-outward displacements of the atoms in the defective region. The H atom is not shown in the figure due to the simplicity reason but it forms the chemical bond with the O(1) atom and is situated along the positive x direction.

closest to the O-H group move away from the O-H complex by about 0.1 Å. The four Ba atoms exhibit the same pattern in their displacements. These atoms displace themselves by approximately 0.04 Å. Displacements of the positively charged

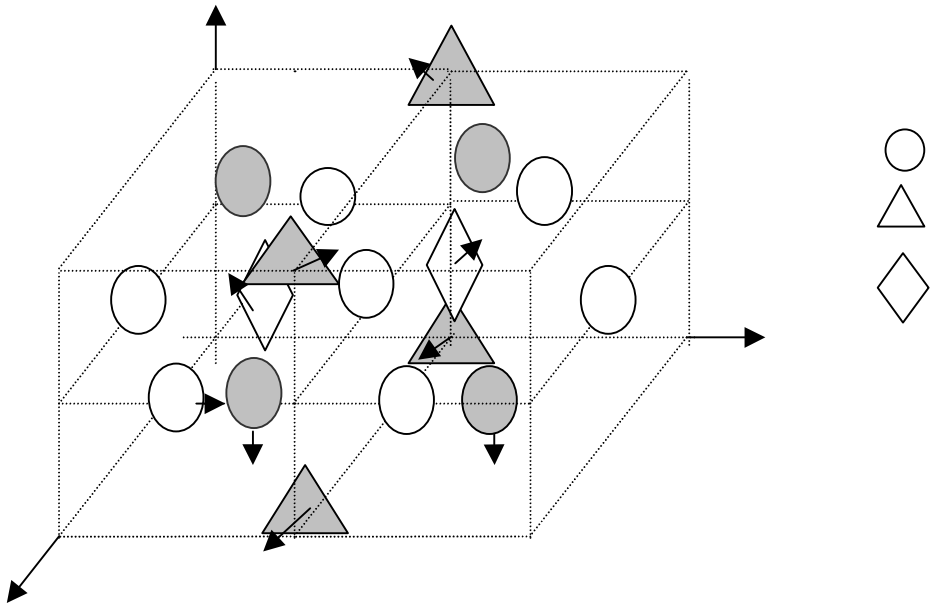

**Fig. 3.** Lattice relaxation in the tetragonal $BaTiO_3$ phase. The arrows show defect-outward displacements of the atoms in the defective region. The component of atomic displacements along the vertical z-axis is considerably larger compared to the same variable in the cubic phase.

defect-surrounding atoms are understood if one considers that the H atom is charged positively and thus due to the Coulomb interaction the Ba and Ti atoms have repulsion with it and move outwards. Additionally, the insertion of the H impurity is also accompanied by a creation of the chemical bond between the hydrogen and one of the O atoms, O(1). Thus the

chemical bonds between the O(1) and its surrounding Ti and Ba atoms are weakened leading to the outward displacements of these atoms.

As one can observe the lattice relaxation in the tetragonal structure of the $BaTiO_3$ crystal shows a similar pattern (Fig. 3), but we obtain somewhat larger component of the displacements along the z-axis, especially for the Ti(1) and Ba(2) atoms (see Fig. 3). We can also mention that the atomic displacements are not radial with respect to geometric center of the system, O-H group, similarly as in the cubic structure.

### 3.3. Electronic properties of the $BaTiO_3$:H

The hydrogen impurity is found to be an auto-ionized positively charged ion since its donor level lies above the conduction band bottom. The utilized Löwdin method for the electron density analysis gives the description shown in Table 1. The impurity-closest Ba atoms practically do not change their effective charges, except the Ba(1) and Ba(2) atoms in the cubic structure. However, we observe considerable charge redistribution for the H-nearest Ti and O atoms. As it follows from the outcome, the Ti atoms tend to become less positive while the O atoms become less negative. This electron density redistribution suggests that the chemical bonding in the vicinity of the H impurity becomes more covalent. This effect is especially obvious in the tetragonal phase of the crystal (see Table 1).

**Table 1.** Charges on atoms in the defective region of the cubic and tetragonal $BaTiO_3$ crystals: perfect crystal (Q1), doped crystal without the lattice relaxation (Q2), and the equilibrium configuration of doped crystal (Q3). Atomic numeration corresponds to the one given in Figs. 2 and 3 for the cubic and tetragonal phases, respectively.

| Atom (cubic) | Q1 (e) | Q2 (e) | Q3 (e) | Atom (tetragonal) | Q1 (e) | Q2 (e) | Q3 (e) |
|---|---|---|---|---|---|---|---|
| Ba(1) | 1.88 | 1.87 | 1.81 | Ba(1) | 1.88 | 1.87 | 1.87 |
| Ba(2) | 1.88 | 1.87 | 1.81 | Ba(2) | 1.88 | 1.87 | 1.86 |
| Ba(3) | 1.88 | 1.88 | 1.88 | Ba(3) | 1.88 | 1.88 | 1.88 |
| Ba(4) | 1.88 | 1.88 | 1.88 | Ba(4) | 1.88 | 1.88 | 1.88 |
| Ti(1) | 2.25 | 1.90 | 2.16 | Ti(1) | 2.02 | 1.84 | 1.85 |
| Ti(2) | 2.25 | 1.91 | 1.70 | Ti(2) | 2.02 | 1.52 | 1.54 |
| O(1) | -1.38 | -1.35 | -1.25 | O(1) | -1.30 | -1.30 | -1.22 |
| O(4) | -1.38 | -1.41 | -1.25 | O(4) | -1.30 | -1.33 | -1.30 |
| O(5) | -1.38 | -1.36 | -1.37 | O(8) | -1.31 | -0.85 | -0.83 |
| H(1) | — | 0.53 | 0.50 | O(9) | -1.31 | -1.27 | -1.29 |
| — | — | — | — | H(1) | — | 0.55 | 0.47 |

### 3.4. Hydrogen effect upon ferroelectric polarization in $BaTiO_3$

An important issue concerning impurities and defects in ferroelectric crystals is their effect on the ferroelectric polarization. The $BaTiO_3$ crystal exhibits the ferroelectricity in its tetragonal phase and that is why we investigated possible bulk ferroelectricity changes due to the H insertion. Our qualitative study shows that the absolute values of the effective charges reduce while the Ti-O bond-lengths increase considerably in the defective region. The first effect tries to reduce while the second effect augments the ferroelectric dipole momentum. A simple calculation shows that the second effect, i.e., the increase of the Ti-O bond-lengths is stronger 1.27 times. This indicates that the direction of the new dipole is favorably aligned with the host polarization. Therefore, one can see augmentation of the ferroelectric polarization in the $BaTiO_3$ crystal due to the H impurity. The well-known loss of ferroelectricity by hydrogen contamination thus *is not a bulk effect*. The primary damage should be localized at the electrode-ferroelectric interface.

### 3.5. Diffusion of the H atom in the cubic $BaTiO_3$ crystal

The diffusion is very important physical process but it is rather difficult to study. We investigated the diffusion in the crystal taking into consideration a number of different trajectories. The trajectory with smaller potential energy barrier was found to be a three-dimensional trajectory having a parabolic form.

### 3.6. H atom in the cubic $CaTiO_3$ crystal

The analysis of obtained results for the H-doped $CaTiO_3$ crystals shows that the interstitial H is found to tie to one of the O atoms forming the O-H group, similarly as in the above-discussed $BaTiO_3$ crystals. At equilibrium, the O-H distance is found to be equal to 0.89 and 1.04 Å for the cubic and orthorhombic lattices, respectively.

Different kinds of atomic relaxations, which included both symmetric and asymmetric atomic displacements, were used to obtain the energy-minimum configuration. The obtained total relaxation energy was found to be 1.1 eV. As a result it was found that the two H-neighboring O atoms located in the parallel plane to the O-H bond (z-axis), move towards the impurity by 0.07 Å (Fig. 4). Thus one can note a shortening of the initial inter-atomic distance, equal to 2.58 Å. This particular relaxation gives about 70.4% of the total relaxation energy. The others H-neighboring O atoms located in the parallel plane to y-axis move towards the H atom by about 0.09 and 0.19 Å along the <111> and <101> directions, respectively. The two H-closest Ti atoms move outwards from the impurity by 0.07 Å, which corresponds to increase of the initial inter-atomic distance between the H and Ti atoms, equal to 1.88 Å. The contribution into the total relaxation energy of the latter is about 12.32%. Finally, the movements of the two nearest Ca atoms were considered. These Ca atoms are located in the same plane with the binding O atom and are situated initially at 2.14 Å from the H impurity. The atomic displacements of the Ca atoms were found to be of 0.1 Å, which contributes with an 8.02% into the total relaxation energy. The detailed information on atomic movements is given in Table 2 and Fig. 4.

**Table 2.** Displacements of atoms, d, and charges on atoms in the defective region of the cubic $CaTiO_3$ crystal: perfect crystal (Q1), doped crystal without the lattice relaxation (Q2), and the equilibrium configuration of doped crystal (Q3). Atomic numeration corresponds to the one given in Fig. 4.

| Atom | d (Å) | Q1 (e) | Q2 (e) | Q3 (e) |
|---|---|---|---|---|
| Ca(11) | 0.31 | 1.89 | 1.88 | 1.88 |
| Ca(36) | 0.18 | 1.89 | 1.88 | 1.88 |
| Ti(2) | 0.05 | 1.55 | 1.75 | 1.76 |
| Ti(12) | 0.13 | 1.86 | 1.80 | 1.91 |
| O(3) | 0.09 | -1.32 | -1.37 | -1.34 |
| O(5) | 0.03 | -1.32 | -1.34 | -1.32 |
| O(10) | 0.05 | -1.32 | -1.33 | -1.33 |
| O(13) | 0.19 | -1.34 | -1.36 | -1.30 |
| O(14) | — | -1.30 | -1.24 | -1.19 |
| H(41) | — | — | 0.44 | 0.41 |

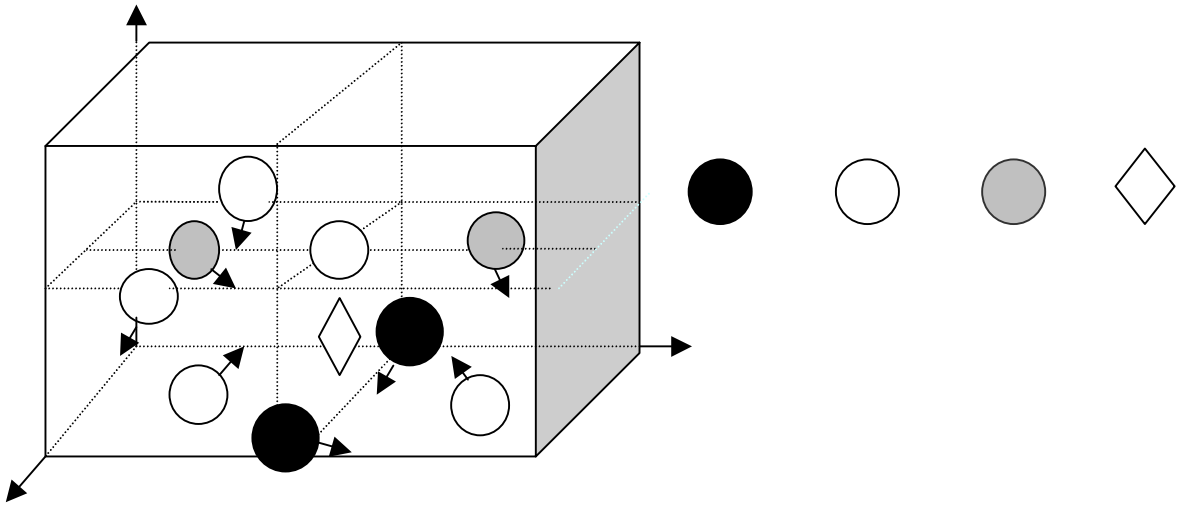

**Fig. 4.** Lattice relaxation in the cubic phase of $CaTiO_3$ crystal. The arrows show atomic displacements in the defective region.

### 3.7. H atom in the orthorhombic $CaTiO_3$ crystal

The atomic relaxation in the orthorhombic phase of H-doped $CaTiO_3$ crystal was made in basis of the analysis for different O positions in the orthorhombic structure, which could participate in the O-H bond creation. In a similar manner as for the cubic phase different kinds of lattice distortion were considered. As a result the total relaxation energy value obtained for this phase was found to be equal to 2.1eV. The three H-closest Ca atoms move toward the impurity by 0.09, 0.18 and 0.37Å

each one, which is about 0.87%, 1.83% and 3.5% of the corresponding initial distances, equal to 2.63, 2.59 and 2.28 Å, respectively (see Fig. 5). The two H-closest Ti atoms move outward from the impurity by 0.09 and 0.37 Å, which represents the 4.71% and 19.27% of the corresponding initial distances, 1.91 and 1.92 Å. These movements are along the <111> directions. The six H-closest O atoms move toward the defect by about 0.09 Å while the H-closest O atom displaces toward the impurity by 0.37 Å. It is worth to be mentioned that the relaxations along both <111> and <101> directions are according to the Coulomb law. The detailed information on atomic movements is given in Table 3 and Fig. 5.

**Table 3.** Initial distances, d1, displacements of atoms, d2, and charges on atoms in the defective region of the orthorhombic $CaTiO_3$ crystal: doped crystal without the lattice relaxation (Q1), and the equilibrium configuration of doped crystal (Q2). Atomic numeration corresponds to the one given in Fig. 5.

| Atom | d1(Å) | d2 (Å) | Q1 (e) | Q2 (e) |
|---|---|---|---|---|
| 1 Ca | 2.6383 | 0.0930 | 1.8738 | 1.8730 |
| 2 Ca | 2.5919 | 0.1857 | 1.8738 | 1.8683 |
| 3 Ca | 2.2852 | 0.3721 | 1.3155 | 1.7058 |
| 1 Ti | 1.9193 | 0.0930 | 2.2473 | 2.1114 |
| 2 Ti | 1.9228 | 0.3721 | 2.1072 | 1.9365 |
| 1 O | 2.6734 | 0.3721 | -1.2132 | -1.1516 |
| 2 O | 2.7275 | 0.0762 | -1.2261 | -1.1297 |
| 3 O | 2.7133 | 0.0930 | -1.1847 | -1.1611 |
| 4 O | 2.7643 | 0.0930 | -1.1847 | -1.2121 |
| 5 O | 2.5928 | 0.0930 | -1.2132 | -1.1168 |
| 6 O | 2.7278 | 0.0930 | -1.5054 | -1.5003 |
| 7 O | 2.6781 | 0.0930 | -1.1847 | -1.1706 |
| 8 O | - | - | -1.5054 | -1.4333 |
| 1 H | 1.9657 | - | - | 0.4833 |

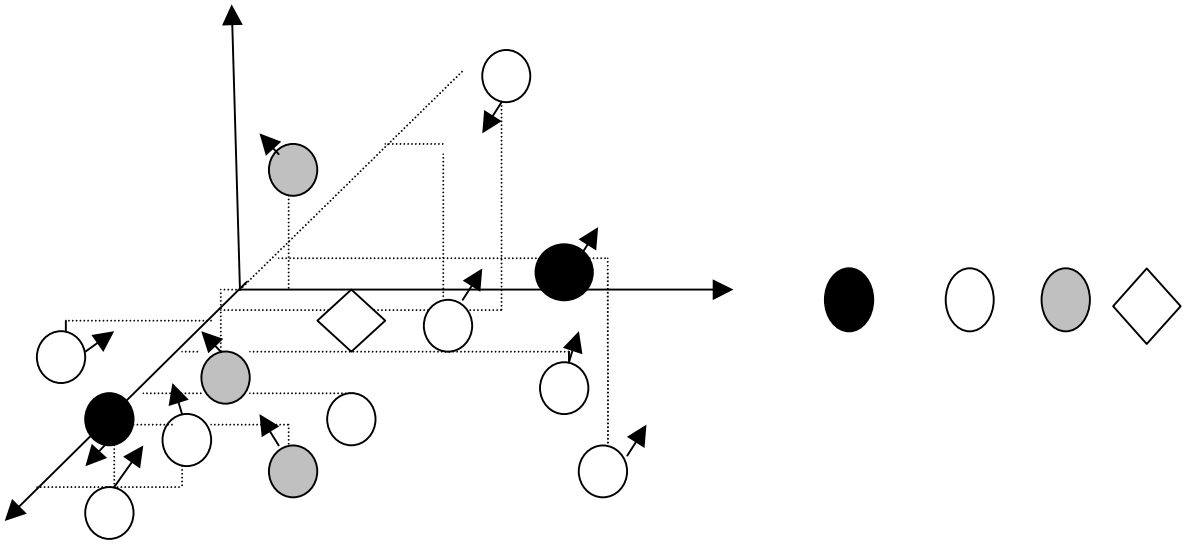

**Fig. 5.** Lattice relaxation in the orthorhombic $CaTiO_3$ phase. The arrows show displacements of atoms in the defective region.

## 4. CONCLUSIONS

In the present work we have studied H-doping in the cubic and orthorhombic lattices of $CaTiO_3$ crystals as well as in the cubic and tetragonal lattices of $BaTiO_3$ crystals using the quantum-chemical method developed for crystal computations. The obtained O-H bond lengths are found to be equal to 0.89 and 0.91 Å in the $BaTiO_3$ cubic and tetragonal phases, respectively. The corresponding values for the cubic and orthorhombic lattices of $CaTiO_3$ crystals are 0.89 and 1.04 Å. Host Ti-O bonds are found to be significantly weakened around the hydrogen impurity. Our study shows that the bulk ferroelectric polarization augments 1.27 times. This may provide an explanation for oxygen loss in ferroelectric films near

the surface under thermal annealing in a hydrogen atmosphere.[25] Oxygen loss is enhanced around defective regions and especially at an interface where the hydroxyl ion can chemically react with the electrode. Damage at the metal/ferroelectric interface can prevent polarization switching and lead to a reduction of the switching charge of the ferroelectric capacitor. As a result of our study we can conclude that the degradation is not a bulk effect since H impurity augments the bulk ferroelectric polarization. Hydrogen diffusion in the cubic $BaTiO_3$ lattice is studied considering different types of trajectories. The trajectory giving the lower potential energy barrier for the H atom movement is found to be of a parabolic form.

## REFERENCES


1. J. Feinberg, D. Heiman, A. R. Tanguay Jr., and R. W. Hellwarth, "Photorefractive effects and light-induced charge migration in barium titanate," *J. Appl. Phys.* **51**, pp. 1296-1305, 1980.
2. E. Krätzig, F. Welz, R. Orlowski, V. Doormann , and M. Rosenkranz, "Holographic storage properties of $BaTiO_3$," *Solid State Commun.* **34**, pp. 817-819, 1980.
3. D. Rytz, B. A. Wechsler, M. H. Garrett , C. C. Nelson, and R. N. Schwartz, "Photorefractive properties of $BaTiO_3$:Co," *J. Opt. Soc. Am. B* **7**, pp. 2245-2254, 1990.
4. Y. Arita, K. Nagarajan, T. Ohashi, and T. Matsui, "Heat capacity measurements on $CaTiO_3$ doped with Ce and La," *J. Nuclear Mater.* **247**, pp. 94-97, 1997.
5. A. L. Shluger and E. V. Stefanovich, "Models of the self-trapped exciton and nearest-neighbor defect pair in $SiO_2$," *Phys. Rev. B* **42**, pp. 9664-9673, 1990.
6. R. A. Evarestov and V. A. Lovchikov, "Large unit cell calculations of solids in the CNDO approximation," *Phys. Status Solidi (b)* **97**, pp. 743-751, 1979.
7. A. Stashans and M. Kitamura, "A study of a hydrogen doped semiconductors using the INDO method," *Solid State Commun*. **99**, pp. 583-588, 1996.
8. S. Lunell, A. Stashans, L. Ojamäe, H. Lindström, and A. Hagfeldt, "Li and Na diffusion in $TiO_2$ from quantum chemical theory versus electrochemical experiment," *J. Am. Chem. Soc*. **119**, pp. 7374-7380, 1997.
9. F. Erazo and A. Stashans, "Quantum-chemical studies of Nb-doped $CaTiO_3$ crystal," *Phil. Mag. B* **80**, pp. 1499-1506, 2000.
10. P. Sánchez and A. Stashans, "Computational study of structural and electronic properties of superconducting La-doped $SrTiO_3$," *Phil. Mag. B* **81**, pp. 1963-1976, 2001.
11. A. Stashans and H. Pinto, "Hole polarons in pure $BaTiO_3$ studied by computer modeling," *Int. J. Quant. Chem.* **79**, pp. 358-366, 2000.
12. A. Stashans and H. Pinto, "Analysis of radiation-induced hole localization in titanates," *Rad. Measurements* **33/35**, pp. 553-555, 2001.
13. H. Pinto and A. Stashans, "Computational study of self-trapped hole polarons in tetragonal $BaTiO_3$," *Phys. Rev. B* **65**, p. 134304, 2002.
14. A. Stashans, "Quantum-chemical studies of free and potassium-bound hole polarons in $SrTiO_3$ cubic lattice," *Mater. Chem. Phys.* **68**, pp. 124-129, 2001.
15. H. Pinto, A. Stashans, and P. Sánchez, *Defects and Surface-Induced Effects in Advanced Perovskites*, NATO Science Series, High Technology, Vol. 77, p. 67, Kluwer Academic Publishers, Dordrecht, 2000.
16. E. Patiño and A. Stashans, "Structural and electronic effects in $BaTiO_3$ due to the Nb doping," *Ferroelectrics* **256**, pp.189-200, 2001.
17. E. Patiño and A. Stashans, "Structural and electronic properties in cubic and tetragonal $BaTiO_3$ crystal due to La impurity," *Comput. Mater. Sci.* **22**, pp. 137-143, 2001.
18. E. Patiño, A. Stashans, and R. Nieminen, "Quantum chemical study of effects produced by Nb- and La-doping in $BaTiO_3$," *Key Engin. Mater.* **206-213**, pp. 1325-1328, 2002.
19. A. Stashans and P. Sánchez, "A theoretical study of La-doping in strontium titanate," *Mater. Lett.* **44**, pp. 153-157, 2000.
20. P. Sánchez and A. Stashans, "Computational studies and comparison of Nb- and La-doped $SrTiO_3$," *Phys. Status Solidi (b)* **230**, pp. 397-400, 2002.
21. F. Erazo and A. Stashans, "Quantum-chemical studies of Nb-doped $CaTiO_3$," *Phil. Mag. B* **80**, pp. 1499-1506, 2000.
22. F. Erazo and A. Stashans, "Structural and electronic properties of La-doped $CaTiO_3$ crystal," *Int. J. Quant. Chem*. **87**, pp. 225-231, 2002.
23. E. Patiño, F. Erazo, and A. Stashans, "Electron transfer effect in $BaTiO_3$ and $CaTiO_3$ due to Nb-doping," *Mater. Lett*. **50**, pp. 337-340, 2001.

24. A. Stashans, C. Zambrano, A. Sánchez, and L. M. Prócel, "Structural properties of $PbTiO_3$ and $PbZr_xTi_{1-x}O_3$: a quantum chemical study," *Int. J. Quant. Chem.* **87**, pp. 145-151, 2002.
25. N. Ikarashi, "Analytical transmission electron microscopy of hydrogen-induced degradation in ferroelectric $Pb(Zr,Ti)O_3$ on a Pt electrode," *Appl. Phys. Lett.* **73**, pp. 1955-1957, 1998.

*Correspondence: Email: corp_ffa@yahoo.com; Fax: +593-2-2401583